CHAPTER 19

Engine Modeling

As discussed in the previous chapter, a key component of picoscopic modeling is to capture vehicle dynamics. Such an issue has been greatly simplified in microscopic modeling where the driver and vehicle are combined into a single unit called an active particle. Vehicle dynamic properties are either ignored or simplified. For example, in steady-state car-following models such as the Pipes model, a vehicle's speed can jump from zero to an arbitrary full speed, resulting in an unrealistic acceleration profile. In dynamic car-following models such as General Motors models, the rate of acceleration can change in such a way that is beyond the capability of real-world vehicles. However, in picoscopic modeling, finer details and accuracy are called for, and hence the above simplified approach becomes inadequate. Because vehicle acceleration plays an important role in traffic operation such as in the calculation safe car-following distances, the determination of acceptable gap sizes, and bypassing slow vehicles, it is critical to base the modeling on sound dynamic vehicle models. Toward this goal, engine modeling is the first step which determines the available power and further torque under varying speeds. Then, the power and torque are fed into dynamic vehicle models to determine the vehicle's acceleration capability.[1]

19.1 INTRODUCTION

Though there has been a wealth of literature in the modeling of internal combustion (IC) engines, these models were developed with a special interest in assisting engine design, analysis, control, and diagnosis. While these models are quite successful for their intended purposes, several reasons prevent them from being equally successful in traffic flow modeling and further the modeling of connected vehicle technology (CVT). For example, a typical procedure in these applications is to invoke routines such as car-following, lane-changing, and gap-acceptance logic to check for potential collisions. To ensure safety, this procedure has to be repeated with such a high frequency that conventional engine models, owing to their intrinsic complexity, are beyond the capacity of a contemporary onboard computer.

[1] This chapter is reproduced from [72].

Traffic Flow Theory
http://dx.doi.org/10.1016/B978-0-12-804134-5.00019-2

In addition, most of these engine models require proprietary parameters such as throttle body size and mass of the piston. This prevents the adoption of these models across a wide variety of vehicles. Therefore, an ideal engine model suited for the above-mentioned applications should meet the following criteria:

- Accuracy: The engine model must provide reasonable accuracy to predict engine performance with throttle and engine speed as inputs and engine power and torque as outputs.
- Computational efficiency: The engine model must be simple enough to facilitate onboard computing with high frequency in real time.
- Accessibility: To assist wide deployment across different vehicles, the engine model should not rely on proprietary parameters and variables that are difficult to obtain. All the information needed to run the model (such as peak engine power, torque, and the associated engine speeds) should be publicly available (e.g., http://www.cars.com).
- Formulation: The engine model should be analytical. Engine models based on lookup tables are not only prohibitive to prepare wide classes of vehicles but are also resource-demanding in computation and storage.
- Calibration: The engine model should involve the least calibration effort or better yet should be calibration-free. Again, it would be a daunting task if an engine model had to be calibrated for every vehicle.

With the above list of criteria, the objective of this chapter is to develop a simple engine model that is suited for these applications. Three simple engine models are presented in this chapter. These engine models will be formulated and empirically validated. Special attention will be paid to the above criteria when we compare the performance of these models, on the basis of which the best model will be recommended. Compared with existing work reviewed in the next section, a limited theoretical contribution is claimed in that these models are rather simple and some of the modeling concepts (such as polynomial fitting and the Bernoulli principle) have already been explored in the past. However, the recommended model does fill a gap in a nonconventional arena such as CVT-enabled applications, where excellent computational efficiency and reasonable accuracy are desirable.

19.2 REVIEW OF EXISTING ENGINE MODELS

The objective of this section is to highlight existing work in engine modeling with an emphasis on IC engines. Given the wealth of literature, it

is practically intractable to include all work. Nevertheless, the review should present a reasonable overview of historical efforts and the current state.

It appears that efforts to model engines have a much shorter history than the engine itself. The first physically based dynamic engine models were reported in Refs. [73–76] which recognized the effects of throttle and intake manifold dynamics. Much of the early effort in engine modeling was surveyed in Ref. [77], with a focus on IC engine models for control.

A trend of increasing modeling accuracy was quite noticeable in the historical evolution. The engine models developed in Refs. [78, 79] included fuel film dynamics and engine rotational dynamics with transport delays. Continuing this modeling approach, a three-state engine model was developed in Ref. [80] based on the work in Refs. [74, 75, 81]. Shortly afterward, Akinci et al. [82] also presented a nonlinear three-state dynamic model of a spark-ignition engine and further effort was reported in Ref. [83]. Rizzoni [84] formulated a global model for the IC engine, and a concurrent paper [85] described a stochastic model. A nonlinear engine model was proposed in Ref. [86]. Hong [87] developed an engine model based on the "filling and emptying" method for unsteady gas flow across the engine cylinder [88]. A low-dimensional, physically motivated engine model was proposed in Ref. [89]. Shiao et al. [90] proposed remedies to the assumption of constant mass moments of inertia which had led many engine models to perform poorly under high engine speed. To serve the purpose of engine design, Chiavola [91] described the unsteady gas flow in both intake and exhaust systems. A very complicated engine model involving 12 degrees of freedom [92] was proposed to capture even more details.

On the applied side, efforts were identified which adopted existing models or extended existing work. Kabganian and Kazemi [93] applied the two-state engine model developed in Ref. [80] to slip control. A real-time engine model [94] similar to that in Ref. [78] was used to develop a nonlinear model-based control strategy for hybrid vehicles. Delprat et al. [95] modeled an IC engine as part of hybrid vehicle modeling. Scillieri et al. [96] developed a direct-injection spark-ignition engine model to demonstrate the potential performance benefits of reference feed-forward control. Two simulation packages involving IC engine models [97, 98] were also identified.

In contrast to the ever-increasing desire for modeling details, some applications such as real-time engine control necessitate simpler engine models. Recognizing the inherently nonlinear nature of IC engines, Cook and Powell [99] argued that a linear engine model reduced from the model

in Ref. [73] might be desirable for the purpose of engine control analysis. To facilitate the development of autonomous intelligent cruise control), Swaroop et al. [100] used an engine model which was essentially the first state equation developed in Ref. [80]. A very simple engine model was presented in Ref. [101] for teaching purposes. An even simpler model was suggested by Genta [102] to assist the modeling of vehicle dynamics, and we shall revisit this model shortly.

To facilitate a cross-comparison of engine models in terms of their complexity, accuracy, accessibility, and intended applications, a summary table is provided in Appendix 19.A.

19.3 SIMPLE MATHEMATICAL ENGINE MODELS

This section presents three simple engine models. Model I is an existing model [102], while models II and III were developed by the author.

19.3.1 Model I: Polynomial Model

In an effort to develop a dynamic vehicle model, Genta [102] suggested a very simple engine model which used a polynomial to empirically approximate the relationship between engine power, P, and engine speed, ω—that is,

$$P = \sum_{i=1}^{3} C_i \omega^i, \tag{19.1}$$

where the C_i ($i = 0, 1, 2, 3$) are coefficients and can be estimated from empirical engine curves. Artamonov et al. [103] suggested the following values for a spark-injection engine:

$$\begin{aligned} C_1 &= P_{\max}/\omega_{\mathrm{p}}, \\ C_2 &= P_{\max}/\omega_{\mathrm{p}}^2, \\ C_3 &= -P_{\max}/\omega_{\mathrm{p}}^3, \end{aligned} \tag{19.2}$$

where $P_{\max}$ is the peak power and $\omega_{\max}$ is the engine speed at which the power peaks. As is well known, engine torque, Γ, is engine power divided by engine speed:

$$\Gamma = \sum_{i=1}^{3} C_i \omega^{i-1}, \tag{19.3}$$

where coefficients C_i ($i = 0, 1, 2, 3$) remain the same as in Equation 19.1.

19.3.2 Model II: Parabolic Model

Motivated by the simplicity of model I and noticing the peak in a typical engine torque curve, one conjectures that a parabola might suffice to approximate the torque curve:

$$\Gamma = C_1 + C_2(\omega - \omega_t)^2, \tag{19.4}$$

where C_1 and C_2 are constants and ω_t is the engine speed at peak torque. To ensure that the power curve peaks at ω_p, one replaces C_1 with a different coefficient C_3:

$$P = C_3\omega + C_2(\omega - \omega_t)^2\omega. \tag{19.5}$$

Given that the engine outputs P_{max} at ω_p and outputs Γ_{max} at ω_t, the following result:

$$\Gamma_{max} = C_1 + C_2(\omega_t - \omega_t)^2 = C_1, \tag{19.6}$$

$$P_{max} = C_3\omega_p + C_2(\omega_p - \omega_t)^2\omega_p, \tag{19.7}$$

$$\frac{dP}{d\omega}|_{\omega=\omega_p} = (C_3 + C_2(\omega - \omega_t)^2 + 2C_2\omega(\omega - \omega_t))|_{\omega=\omega_p} = 0. \tag{19.8}$$

Solve Equations 19.7 and 19.8:

$$C_2 = -\frac{P_{max}}{2\omega_p^2(\omega_p - \omega_t)}, \tag{19.9}$$

$$C_3 = \frac{P_{max}}{2\omega_p^2}(3\omega_p - \omega_t). \tag{19.10}$$

Therefore,

$$\Gamma = \Gamma_{max} - \frac{P_{max}}{2\omega_p^2(\omega_p - \omega_t)}(\omega - \omega_t)^2, \tag{19.11}$$

$$P = \frac{P_{max}}{2\omega_p^2}(3\omega_p - \omega_t)\omega - \frac{P_{max}}{2\omega_p^2(\omega_p - \omega_t)}(\omega - \omega_t)^2\omega. \tag{19.12}$$

Equations 19.11 and 19.12 constitute model II, and guarantees that its power and torque curves peak at their respective peak engine speeds.

19.3.3 Model III: Bernoulli Model

This model is based on the Bernoulli principle, which states that for an ideal fluid (e.g., air) on which no external work is performed, an increase in velocity occurs simultaneously with a decrease in pressure or a change in the fluid's gravitational potential energy. When the fluid flows through a pipe

(e.g., the intake manifold) with a constriction (e.g., the throttle) in it, the fluid velocity at the constriction must increase in order to satisfy the equation of continuity, while its pressure must decrease because of conservation of energy. The limiting condition of this effect is choked flow, where the mass flow rate is independent of the downstream pressure (e.g., in the combustion chamber), depending only on the temperature and pressure on the upstream side of the constriction (e.g., the atmosphere). The physical point at which the choking occurs is when the fluid velocity at the constriction is at sonic conditions or at a Mach number (the ratio of fluid velocity and sound speed) of 1. With the above knowledge, the Bernoulli engine model is developed as follows.

The theoretical volumetric fresh mixture flow rate into the engine, $\dot{V}_t$, is

$$\begin{aligned}\dot{V}_t\ (\mathrm{m}^3/\mathrm{s}) &= V_e\ (\mathrm{m}^3/\mathrm{cycle})\ \times \text{cycles/revolution} \\ &\quad \times \text{enginespeed(revolutions/s)},\end{aligned} \tag{19.13}$$

where V_e is engine displacement, the number of cycles per revolution is 1/2 for a four-stroke engine, and the engine speed (revolutions per second) is $\omega_e/2$, where ω_e is the engine speed in radians per second. Therefore,

$$\dot{V}_t = V_e \times \frac{1}{2} \times \frac{\omega}{2\pi} = \frac{V_e \omega_e}{4\pi}. \tag{19.14}$$

This model assumes that the air is an ideal gas. According to the ideal gas law,

$$pV = \frac{m}{m'} RT, \tag{19.15}$$

where p is the absolute pressure, V is the volume of the vessel containing the gas, m is the mass of the gas, m' is the molar mass of the gas, R is the gas constant, and T is the temperature in kelvins. Therefore, $m = \frac{pm'V}{RT}$, and the density of the gas in the vessel is

$$\rho = \frac{m}{V} = \frac{pm'}{RT} = \frac{p}{R_a T}, \tag{19.16}$$

where $R_a = R/m'$ and for air $R_a \approx 287$ N m/kg/K. Further, the mass air flow rate, $\dot{m}$, as a function of the volumetric air flow rate, $\dot{V}$, is

$$\dot{m} = \frac{pm'}{RT} \dot{V} = \frac{p}{R_a T} \dot{V}. \tag{19.17}$$

For an engine, $\dot{V}$ is replaced by $\dot{V}_t$ and the speed of air flow is $v = \dot{V}/A$, where A is the cross-sectional area of any point in the intake manifold. The

constriction in the manifold is the throttle, whose cross-sectional area is $\theta \times A$, where θ is percent of throttle opening. So the mass flow rate of air entering the engine is

$$\dot{m} = \frac{p}{R_a T}\dot{V}_t = \frac{p}{R_a T} vA. \tag{19.18}$$

According to compressible fluid mechanics [104], the speed of air flow, v, is related to a Mach number, M_a, which is the ratio of air flow speed to sound speed $v_s = \sqrt{kR_a T}$—that is,

$$M_a = \frac{v}{v_s} = \frac{v}{\sqrt{kR_a T}} = \frac{\dot{V}_t}{A\sqrt{kR_a T}}, \tag{19.19}$$

where k is the specific heat ratio. Assume the stagnation state (where the flow is brought into a complete motionless condition in an isentropic process without other forces) holds. With the stagnation state for the ideal gas model in Sections 4.1 and 4.2 in Ref. [104], Equation 19.18 can be translated to

$$\dot{m} = A\left(\frac{\sqrt{k}M_a p_0}{\sqrt{R_a}T_0}\right)\left(1 + \frac{k-1}{2}M_a^2\right)^{-\frac{k+1}{2(k-1)}}, \tag{19.20}$$

where p_0 and T_0 are the stagnation pressure and temperature, respectively. Plugging 19.19 into 19.20 yields

$$\dot{m} = A\left(\frac{\dot{V}_t p_0}{AR_a T_0}\right)\left(1 + \frac{\dot{V}_t^2(k-1)}{2A^2 kR_a T_0}\right)^{-\frac{k+1}{2(k-1)}}. \tag{19.21}$$

Notice that Equations 19.20 and 19.21 apply to flow everywhere. When the flow is choked (i.e., $M_a = 1$) and the stagnation conditions (i.e., temperature, pressure) do not change, Equation 19.20 reduces to

$$\dot{m} = A\left(\frac{\sqrt{k}p_0}{\sqrt{R_a}T_0}\right)\left(1 + \frac{k-1}{2}\right)^{-\frac{k+1}{2(k-1)}}. \tag{19.22}$$

For exact stoichiometric air-fuel ratio λ, fuel energy density E_f, and engine thermal efficiency η, the power developed by the engine is

$$P = \lambda E_f \eta\left[A\left(\frac{\dot{V}_t p_0}{AR_a T_0}\right)\left(1 + \frac{\dot{V}_t^2(k-1)}{2A^2 kR_a T_0}\right)^{-\frac{k+1}{2(k-1)}}\right]. \tag{19.23}$$

Plugging in equation 19.14, we obtain

$$P = \lambda E_f \eta \left[A \left(\frac{V_e \omega_e p_0}{4\pi A R_a T_0} \right) \left(1 + \frac{V_e^2 \omega_e^2 (k-1)}{32\pi^2 A^2 k R_a T_0} \right)^{-\frac{k+1}{2(k-1)}} \right]. \quad (19.24)$$

The torque that the engine develops is

$$\Gamma = \lambda E_f \eta \left[A \left(\frac{V_e p_0}{4\pi A R_a T_0} \right) \left(1 + \frac{V_e^2 \omega_e^2 (k-1)}{32\pi^2 A^2 k R_a T_0} \right)^{-\frac{k+1}{2(k-1)}} \right]. \quad (19.25)$$

Empirical comparison shows that this model explains engine performance quite well up to peak torque and power. However, there are considerable differences between the model and the empirical engine curves after peak torque and power. Therefore, the engine model is modified by the addition of a correction term:

$$P = \lambda E_f \eta \left[A \left(\frac{V_e \omega_e p_0}{4\pi A R_a T_0} \right) \left(1 + \frac{V_e^2 \omega_e^2 (k-1)}{32\pi^2 A^2 k R_a T_0} \right)^{-\frac{k+1}{2(k-1)}} \right] - \alpha P_{\max} e^{\frac{\beta(\omega - \omega_p)}{\omega_p}}, \quad (19.26)$$

where α and β are coefficients to be calibrated. The specific form of the correction term is obtained mainly by trial and error from fitting a wide variety of engine power curves. This model, because of its simplicity, captures only the major aspect of an engine. Since many of the engine details are left out, the model exhibits only moderate accuracy even with the correction term. We also recognize that the concept of this Bernoulli principle—based model is not new, and a similar discussion can be found in existing work, such as [105].

19.4 VALIDATION AND COMPARISON OF THE ENGINE MODELS

To validate the three engine models as well as to compare their relative performance, we need empirical engine power and torque curves. Unfortunately, we do not have much choice because such empirical data are typically proprietary unless they are made available by interested parties. Provided in this validation study are empirical curves for the following four automotive engines: 2008 Mercedes CLS, 2006 Honda Civic, 2006 Pagani Zonda, and 1964 Chevrolet Corvair. Hopefully, these engines provide a good representation of vehicle makes, models, and model years. Technical specifications of these engines are listed in Table 19.1. Additional

Table 19.1 Technical specifications of engines used in the validation study

Engine Tech specification	Mercedes CLS 2008	Honda Civic 2006	Pagani Zonda 2006	Chevrolet Corvair 1964
Peak power (kW)	286	103	408	84
ω at peak power (rpm)	6000	6300	5900	4400
Peak torque (N m)	531	174	750	209
ω at peak torque (rpm)	4000	4300	4050	2800
Engine volume (L)	5.46	1.80	7.30	2.68
Compression ratio	10.7:1	10.5:1	10:1	9.25:1
Throttle diameter (mm)	50*	60	80*	58

*Value is estimated.

information regarding parameter values used in this study is provided in Appendix 19.B.

The primary criterion to evaluate these models is their accuracy. Figures 19.1–19.4 illustrate the relative performance of the three models with use of the empirical engine data as a benchmark. Each figure pertains to one of the engines and consists of two plots—one for power and the other for torque. In principle, the torque curve should contain the same information as the power curve because power is simply the product of torque and engine speed. However, many empirical torque curves exhibit some differences from what their expected form, so both power and torque curves are included here for complete information.

In Figure 19.1, model II fits the empirical power curve very well. Model III also fits well except for the peak power. Model I meets the peak power but overestimates the remaining part of the empirical curve. In terms of torque, model II meets the peak torque but generally falls under the empirical curve. Model III would give a better fit if it were shifted slightly to the left. Model I generally deviates from the empirical curve by a shift to the left and translation upward.

Figure 19.2 generally shows about the same pattern as that in Figure 19.1, with more noticeable deviations for models I and III. Though model II agrees with the peak torque, the model does not fit the empirical torque curve well under very low and very high engine speeds.

In Figure 19.3, model II generally fits the empirical curves well except for the depressed parts under low to middle engine speeds. Model III's torque curve drops too fast after the peak torque. Model I increasingly deviates from the empirical curves as engine speed decreases.

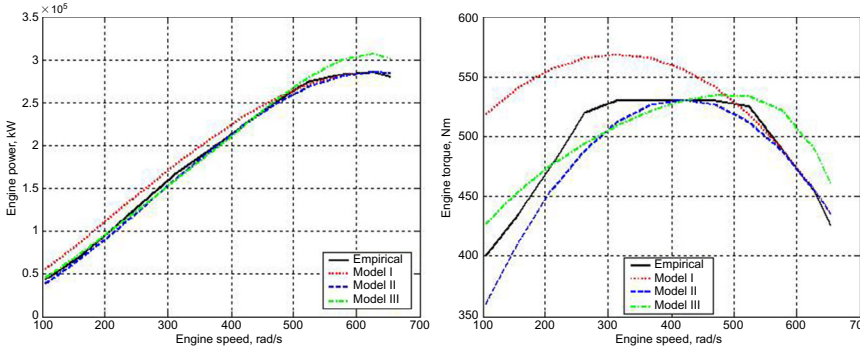

Figure 19.1 Model comparison based on the 2008 Mercedes CLS engine.

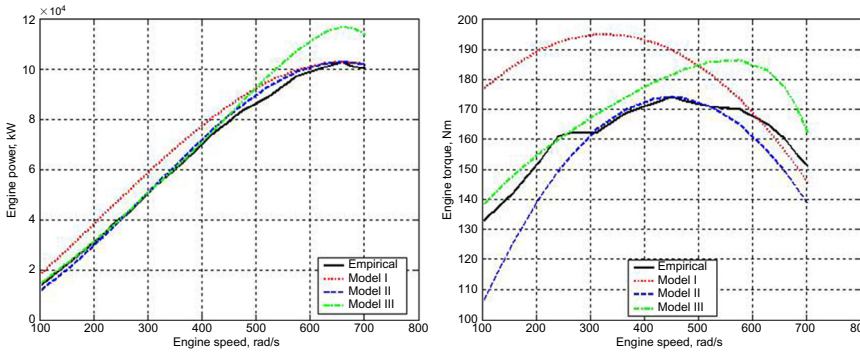

Figure 19.2 Model comparison based on the 2006 Honda Civic engine.

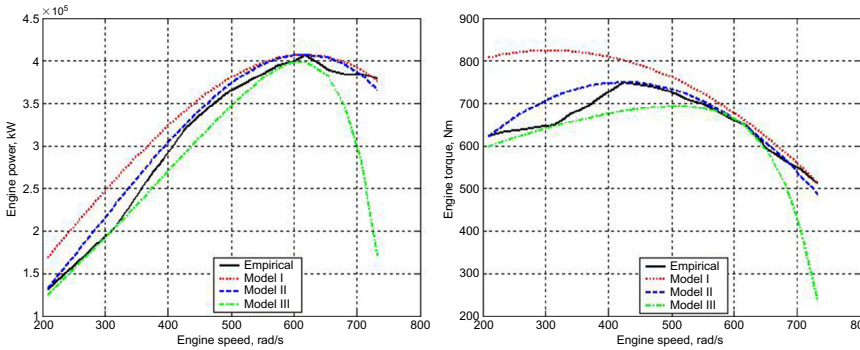

Figure 19.3 Model comparison based on the 2006 Pagani Zonda engine.

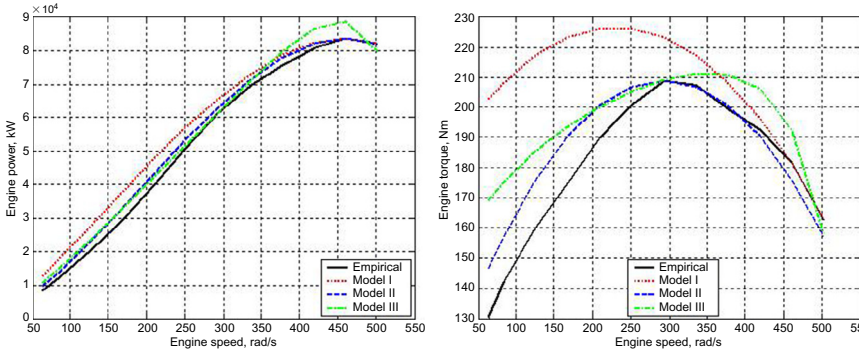

Figure 19.4 Model comparison based on the 1964 Chevrolet Corvair engine.

In Figure 19.4, model II generally overestimates the torque before the peak torque. Except for a good fit of the peak torque, models I and III generally overestimate the torque.

To quantify the accuracy of the three models, the mean absolute percentage error (MAPE) is used as the measure of effectiveness. The MAPE is calculated as

$$\text{MAPE} = \frac{1}{n}\sum_{i=1}^{n}\frac{Y_i - X_i}{Y_i}, \tag{19.27}$$

where n is number of samples, X_i is the model estimate, and Y_i is the corresponding empirical value. Figure 19.5 confirms that model II performs consistently well in both power and torque across the four engines. Its MAPE generally ranges between 3% and 7%. Though less well than model II, model III generally performs quite well, and its MAPE ranges between 4% and 9%. Model I performs the least well of the three models, and its MAPE can be as high as 18%.

The second criterion to evaluate these models is accessibility—that is, the involvement of proprietary parameters and difficult-to-measure variables. In this regard, models I and II are excellent because all they need are peak power and torque and the associated engine speeds. Such information is readily available on the Internet. Model III requires the throttle body diameter, a proprietary parameter, which is less desirable. The third criterion is computational efficiency/model complexity. On average, models I and II consume about 3.2×10^{-5} CPU time to complete a run, while model III takes 0.075 CPU time. Though these numbers appear negligible, the difference is pronounced in real-time applications, especially

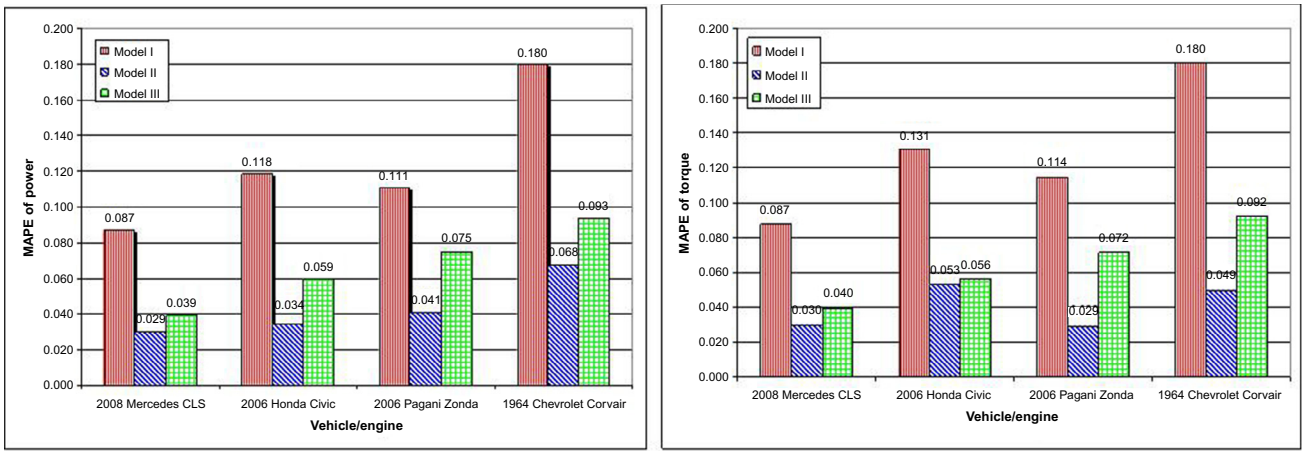

Figure 19.5 MAPE of the three models (left, power; right, torque).

where a procedure has to be repeated very frequently. In terms of the fourth criterion—formulation—all three models are analytical, so no lookup table is involved. The fifth criterion is the need for calibration. In this regard, models I and II involve minimal calibratio—all they need are peak power and torque and the associated engine speeds. Calibration of model III is quite involved owing to its proprietary parameter and calibration coefficients. The above comparison results are also highlighted in Appendix 19.A. Overall, model II outperforms the other two models in terms of the above-mentioned evaluation criteria.

19.5 CONCLUSION

An ideal engine model suitable for in-vehicle applications such as a cooperative driving assistance system is expected to have reasonable accuracy, excellent computational efficiency, high accessibility, an analytical formulation, and little need for calibration. Toward these goals, this chapter has presented three simple engine models: model I is an existing one, and models II and III were developed by the author. These models were formulated, validated, and evaluated. In terms of accuracy, models II and III have moderate accuracy, while model I has low accuracy. In terms of computational efficiency, the three models are all acceptable, with models I and II being particularly efficient. In terms of accessibility, models I and II are excellent because they do not require any proprietary parameter or difficult-to-measure variable. All three models are equally good in terms of analytical formulation. Model III requires much effort for calibration, while models I and II involve minimal calibration. Overall, model II appears the best among the three models in terms of all the evaluation criteria.

19.A A CROSS-COMPARISON OF ENGINE MODELS

19.B PARAMETER VALUES

Engine efficiency $\eta = 0.29$
Fuel energy density $E_f = 46900000$ J/kg
Stoichiometric air-fuel ratio $\lambda = 0.068$
Air density $\rho = 1.29$ kg/m^3
Atmospheric pressure $p = 101325$ Pa
$\pi = 3.14159$
Heat capacity ratio of ideal gas $k = 1.407$
Molar mass of air $m' = 28.9$

Model	Accuracy	Complexity	Accessibility	Applications
I [102]	Low	Low	High	Vehicle dynamics
II	Moderate	Low	High	CVT-enabled in-vehicle control
III	Moderate	Moderate	Moderate	Vehicle dynamics
[101]	Low	Low	Moderate	Vehicle dynamics
[100]	Moderate	Low	Low	Autonomous cruise control
[99]	Moderate	Moderate	Low	Engine control analysis
[73–75]	Moderate	Moderate	Low	Engine control analysis
[78, 79]	High	High	Low	Engine control algorithms
[80]	High	High	NA	Powertrain controllers and dynamics
[82]	High	High	Low	Electric throttle control algorithm
[83]	High	High	Low	Air-fuel ratio control and speed control
[90]	High	High	Low	Engine diagnostics and control
[91]	High	High	Low	The design procedure for IC engines
[92]	High	Very high	Low	Upfront design of engines for noise and vibration targets

Universal gas constant $R = 8314.5$ (N m)/(mol K)
Coefficients in model III, $\alpha = 0.15$ and $\beta = 10$

PROBLEMS

1. State at least three criteria that you would use to evaluate an engine model.
2. Do an Internet search on manufacturer specifications for the 2016 Volvo XC90 engine and find its peak power and torque as well as the corresponding engine speeds. Use the above information to determine the parameters in Section 19.3.1 (model I) and write the specific functional form of power.
3. Use the result from problem 2 to determine the specific functional form of torque and check whether its peak condition matches the manufacturer specification from an Internet search.
4. Use the results of the Internet search in problem 2 to determine the parameters in Section 19.3.2 (model II) and write the specific functional form of power and torque.

5. Verify if the peak power and torque conditions predicted by the model in problem 4 indeed match those of the manufacturer's specifications.
6. Use the results of the Internet search in problem 2 as well as information in Appendices 19.A and 19.B to determine the parameters in Section 19.3.3 (model III) for the 2016 Volvo XC90 engine. Assume a throttle diameter of 70 mm, engine displacement $V_e = 0.002\,m^3$, stagnation pressure $p_0 = 101.325\,kPa$, and stagnation temperature $T_0 = 293.15\,K$.